

**The ^3He Flux Gauge in the Sargasso Sea: a Determination of Physical Nutrient Fluxes to
the Euphotic Zone at the Bermuda Atlantic Time Series Site**

R.H.R. Stanley^{1,2}, W.J. Jenkins², S.C. Doney², and D. E. Lott², III

¹ Department of Chemistry

Wellesley College,

Wellesley, MA 02481

rachel.stanley@wellesley.edu

²Department of Marine Chemistry and Geochemistry

Woods Hole Oceanographic Institution

Woods Hole, MA 02543

1

2 **Abstract:**

3 Significant rates of primary production occur in the oligotrophic ocean, without any measurable
4 nutrients present in the mixed layer, fueling a scientific paradox that has lasted for decades. Here,
5 we provide a new determination of the annual mean physical supply of nitrate to the euphotic
6 zone in the western subtropical North Atlantic. We combine a three year time-series of
7 measurements of trituigenic ^3He from 2003 to 2006 in the surface ocean at the Bermuda Atlantic
8 Time-series Study (BATS) site with a sophisticated noble gas calibrated air-sea gas exchange
9 model to constrain the ^3He flux across the sea-air interface, which must closely balance the
10 upward ^3He flux into the euphotic zone. The product of the ^3He flux and the observed subsurface
11 nitrate- ^3He relationship provides an estimate of the minimum rate of new production in the
12 BATS region. We also apply the gas model to an earlier time series of ^3He measurements at
13 BATS in order to recalculate new production fluxes for the 1985 to 1988 time period. The
14 observations, despite an almost three-fold difference in the nitrate- ^3He relationship, yield a
15 roughly consistent estimate of nitrate flux. In particular, the nitrate flux from 2003-2006 is
16 estimated to be $0.65 \pm 0.14 \text{ mol m}^{-2} \text{ y}^{-1}$, which is ~40% smaller than the calculated flux for the
17 period from 1985-1988. The difference in nitrate flux between the time periods, which is barely
18 significant, may be signifying a real difference in new production resulting from changes in
19 subtropical mode water formation. Overall, the nitrate flux is larger than most estimates of export
20 fluxes or net community production fluxes made locally for the BATS site, which is likely a
21 reflection of the larger spatial scale covered by the ^3He technique and potentially also by
22 decoupling of ^3He and nitrate during obduction of water masses from the main thermocline into

the upper ocean. The upward nitrate flux is certainly large enough to support observed rates of primary production at BATS and more generally in the oligotrophic subtropical ocean.

1. Introduction

Primary production in the subtropical oligotrophic gyres has been an active area of study for decades. In particular, scientists have long puzzled over the seemingly paradoxical drawdown of summertime dissolved inorganic carbon despite no visible source of nutrients (Michaels et al., 1994). Numerous studies using geochemical tracers, sediment traps, and bottle incubations have been performed at the Bermuda Atlantic Time-Series Study (BATS) site over the past several decades (e.g. Brew et al., 2009; Jenkins and Doney, 2003; Jenkins and Goldman, 1985; Spitzer and Jenkins, 1989; Gruber et al., 1998; Stanley et al., 2012; Stewart et al., 2011; Buesseler et al., 2008; Maiti et al., 2009; Maiti et al., 2012; Owens et al., 2013; Lomas et al., 2010), in order to quantify various aspects of biological production and to shed light on this enigma. Floating sediment traps give a direct measure of export production but may be biased by collection efficiency due to hydrodynamic biases and swimmers (Buesseler, 1991), as well as by the limited amount of time they are in the water. Bottle incubations, although primarily used to determine net primary production (Marra, 2002, 2009), can also be conducted to give determinations of new production when conducted with ^{15}N (Dugdale et al., 1992). Bottle incubations give useful information but may be limited by so-called bottle effects of constraining organisms to a bottle (Peterson, 1980; Harrison and Harris, 1986; Scarratt et al., 2006). Geochemical tracers give large scale averages of rates of new production, net community production, or export production.

1 These rates, however, can be difficult to interpret since quantitative interpretation of the tracer
2 data often depends on estimates of physical transport. Thus it is useful to calculate rates of
3 production using numerous approaches and to compare them.

4 One approach that has been used before in the Sargasso Sea is to estimate a lower bound of
5 new production by calculating the upward physical nutrient flux (Jenkins and Doney,
6 2003;Jenkins, 1988b). The global inventory of natural tritium has been dwarfed by the
7 production of so-called “bomb tritium” that was created during the atmospheric nuclear weapons
8 tests in the 1950s and 1960s (Weiss and Roether, 1980). This tritium was deposited in large part
9 in the northern hemisphere (Doney et al., 1992;Stark et al., 2004) and has subsequently entered
10 the oceanic thermocline and abyss by subduction, water mass formation, mixing, and advection
11 (e.g., Rooth and Ostlund, 1972;Ostlund et al., 1974;Broecker and Peng, 1980). Tritium, which
12 has a half-life of 12.31 years (MacMahon, 2006), decays to ^3He , a stable, inert, and rare isotope
13 of helium. Over the decades since the bomb-transient, a significant inventory of this isotope has
14 accrued within the main thermocline of the North Atlantic. There is evidence of an efflux of this
15 isotope via gas exchange from the surface ocean (Jenkins, 1988c, a). Inasmuch as this tritiogenic
16 excess ^3He has a nutrient-like distribution in the thermocline – it is small in the surface ocean
17 due to gas exchange loss and reaches a maximum within the thermocline due to *in situ* tritium
18 decay – it is tempting to argue that the physical return of this isotope to the shallow ocean can be
19 used as a “flux gauge” to determine the rate of physical nutrient supply to the euphotic zone
20 (Jenkins, 1988a;Jenkins and Doney, 2003). Here we report the results of a three year time-series
21 of helium isotope measurements taken approximately monthly between 2003 and 2006 in the
22 surface ocean near Bermuda that allow another determination of this nutrient flux. We compare
23 the calculated nutrient flux to the nutrient flux determined at the same location using the same

method for the period of 1985 to 1998, as well as to export production fluxes calculated in the Sargasso Sea for the time period of 2003 to 2006.

2. Methods

2.1 Data Collection

Samples for ^3He , a suite of noble gases, and tritium were collected at the BATS site (31.7 °N, 64.2°W) on core BATS cruises at approximately monthly resolution between April 2003 and April 2006. The BATS site, located in the subtropical North Atlantic, is representative of a typical oligotrophic gyre. Much biogeochemical research has occurred at that site, because of the long-standing time-series located there (Lomas et al., 2013). In particular, as part of the regular time-series, export fluxes are estimated monthly from surface-tethered floating, upper-ocean sediment traps (Lomas et al., 2010) and rates of net primary production are estimated monthly from radiocarbon bottle incubations (Steinberg et al., 2001). In addition, other researchers have measured export using ^{234}Th (Maiti et al., 2009), neutrally buoyant sediment traps (Owens et al., 2013), or apparent oxygen utilization rates (Stanley et al., 2012; Jenkins, 1980). Net community production has been estimated from the seasonal accumulation of O_2/Ar (Spitzer and Jenkins, 1989) and the drawdown of dissolved inorganic carbon (Gruber et al., 1998; Brix et al., 2006; Fernandez-Castro et al., 2012). New production has been estimated from bottle incubations (Lipschultz, 2001; Lipschultz et al., 2002) and has also been studied using nitrogen isotopes (Fawcett et al., 2014; Knapp et al., 2008).

1 The ^3He and noble gas samples for this study were collected from Niskin bottles by gravity
2 feeding through tygon tubing into valved 90 mL stainless steel cylinders. Typically 22 samples
3 were collected within the upper 400 m, and thus depending on mixed layer depth, there were
4 usually several samples collected within the mixed layer. Within 24 hours of sampling, the gas
5 was extracted from the water stored in the cylinders into ~30 ml aluminosilicate glass bulbs. The
6 bulbs were then brought to the Isotope Geochemistry Facility at WHOI where they were
7 analyzed for ^3He , ^4He , Ne, Ar, Kr, and Xe using a dual mass spectrometric system with the ^3He
8 being analyzed by a magnetic sector mass spectrometer and the other noble gases being analyzed
9 by a quadrupole mass spectrometer (Stanley et al., 2009a). In particular, the magnetic sector
10 mass spectrometer for ^3He measurements was a purposefully constructed, branch tube, statically
11 operated, dual collector instrument equipped with a Faraday cup and a pulse counting secondary
12 electron multiplier. Precision of the ^3He measurements, based on duplicates, was 0.15%. The
13 focus of this paper is on the ^3He measurements, but the other noble gases were used to calculate
14 gas exchange fluxes (Stanley et al., 2009b), which is an important term in the calculation of ^3He
15 flux from the ^3He data.

16 Samples for tritium were collected from the same Niskins by gravity feeding through tygon
17 tubing into 500 mL argon-filled flint glass bottles, as described in Stanley et al. (2012). The
18 tritium samples were degassed at the Isotope Geochemistry Facility at WHOI (Lott and Jenkins,
19 1998), and then the resulting ^3He ingrowth was measured on a purposefully constructed, branch
20 tube dual collector magnetic sector mass spectrometer (a different one than the one used above
21 for ^3He samples). The resulting tritium concentrations were used to correct for tritium ingrowth
22 in the ^3He samples between time of collection and time of measurement (see Sec 3.3).

2.2 Calculation of fluxes

The nitrate flux was calculated in a similar way as is described in Jenkins and Doney (2003). The most notable difference was that in this study the dynamic solubility equilibrium value of ^3He was modeled taking both solubility and bubble injection into account, as described in more detail below. To calculate the nitrate flux, first a ^3He flux was calculated and then the slope of the nitrate: ^3He ratio was applied. The ^3He flux was calculated from the gas exchange parameterization of Stanley et al., (2009b), which had been devised specifically from the noble gas samples collected at the same time as the ^3He samples and thus is well suited to the study site and sampling conditions. In particular, the ^3He flux ($F_{\text{He}3}$) was calculated as the product of a gas transfer velocity k , as determined in Stanley et al. (2009b), and the difference in concentration between the measured ^3He concentration (C) and the dynamic solubility equilibrium value (C_{eq}):

$$F_{\text{He}3} = k * (C - C_{eq}) \quad (1)$$

The dynamic solubility equilibrium refers to the value of $\delta^3\text{He}$ that would be observed in the ocean if the atmosphere was in equilibrium with the water – this is governed by the Henry's law constant for ^3He vs. ^4He (i.e. the fractionation associated with solubility) as well as the fractionating effect of gas exchange including bubble processes on the ratio of ^3He and ^4He . Thus the dynamic solubility equilibrium is the required saturation state such that diffusive gas exchange will balance the bubble effects, in a quasi-steady state system. Laboratory experiments have determined the isotope effect in solution for helium in water as a function of temperature (Benson and Krause, 1980). Given that the helium isotope ratio may be further affected by isotopic fractionation in molecular diffusion (Bourg and Sposito, 2008) associated with the balance between wave-induced bubble trapping and air-sea exchange (Fuchs et al., 1987; Jenkins,

1988b) we have used our observations of the full suite of noble gases on these samples to develop a much more complete model of this dynamic equilibrium isotope effect. Thus the dynamic solubility equilibrium value for ^3He , C_{eq} , was determined by adding ^3He isotopes to a one dimensional Price-Weller-Pinkel (PWP) model (Price et al., 1986) forced by 6 hourly NCEP reanalysis forcing (Kalnay et al., 1996) and QuikSCAT winds from the BATS site (Stanley et al., 2006; Stanley et al., 2009b). The model used the temperature dependent solubility of ^3He from Benson and Krause (1980) and the molecular diffusivity value from Bourg and Sposito (2008). The calculated dynamic solubility equilibrium is sensitive to the amount of air injection, and thus the other noble gases were used to constrain the air injection (Stanley et al., 2009b) (subsequently referred to as S09). In particular, the dynamic solubility equilibrium was calculated including the effects of diffusive gas exchange, partially trapped bubbles, and completely trapped bubbles according to the following equations, described in full in S09.

The diffusive gas exchange flux of ^3He (or another gas such as ^4He) (in units of $\text{mol m}^{-3} \text{s}^{-1}$) was calculated as:

$$F_{GE} = \gamma_G \cdot 8.6 \times 10^{-7} \left(\frac{Sc}{660} \right)^{-0.5} u_{10}^2 (C_{i,eq} - C_{i,w}) \quad (2)$$

where γ_G is an order one, tunable model parameter that scales the magnitude of diffusive gas exchange, Sc is the Schmidt number of the gas (i.e., ^3He), u_{10} is the wind speed in m s^{-1} at a height of 10 m above the sea surface, $C_{i,eq}$ is the concentration of the gas at equilibrium (mol m^{-3}), and $C_{i,w}$ is the concentration of the gas in the water (mol m^{-3}). For QuikSCAT winds, $\gamma_G = 0.97$ and for NCEP winds $\gamma_G = 0.7$.

The flux of ^3He (or other gas) due to completely trapped bubbles was calculated as:

$$F_C = 9.1 \times 10^{-11} (u_{10} - 2.27)^3 \frac{P_{i,a}}{RT} \quad (3)$$

where $P_{i,a}$ is the partial pressure of the gas (i.e. ^3He) in the atmosphere calculated from the fractional abundance of the gas and the variable total atmospheric pressure (Pa), R is the gas constant ($8.31 \text{ m}^3 \text{ Pa mol}^{-1} \text{ K}^{-1}$), and T is the temperature (K).

The flux of ^3He (or another gas) (in units of $\text{mol m}^{-3} \text{ s}^{-1}$) due to partially trapped bubbles was calculated as:

$$F_p = 2.2 \times 10^{-3} \cdot (u_{10} - 2.27)^3 \alpha_i \left(\frac{D_i}{D_o} \right)^{\frac{2}{3}} \frac{(P_{i,b} - P_{i,w})}{RT} \quad (4)$$

where α is the Bunsen solubility coefficient of the gas (Benson and Krause, 1980 for ^3He), D_i is the diffusivity coefficient (for ^3He determined with fractionation factor from Bourg and Sposito (2008) and diffusivity coefficient of Jahne (1987)), D_o is a normalization factor equal to 1 which is included in order to simplify the units ($\text{m}^2 \text{ s}^{-1}$), $P_{i,b}$ is the pressure of the gas in the bubble (Pa) and $P_{i,w}$ is the partial pressure of the gas in the water (Pa).

$P_{i,b}$ is approximated by

$$P_{i,b} = X_i (P_{\text{atm}} + \rho g z_{\text{bub}}) \quad (5)$$

where X_i is the mole fraction of the gas in dry air, P_{atm} is the atmospheric pressure of dry air (Pa), ρ is the density of water (kg m^{-3}), g is the gravitational acceleration (9.81 m s^{-2}), and z_{bub} is the depth to which the bubble sinks (m), which is parameterized, according to Graham et al. (2004):

$$z_{\text{bub}} = (0.15 \cdot u_{10} - 0.55) \quad (6)$$

The main numbers reported in this paper (i.e. the total nitrate flux of $0.65 \text{ mol m}^{-2} \text{ y}^{-1}$), were calculated using the S09 parameterization as described above by Equations 2 to 6 since it was derived from a noble gas time-series collected concurrently with the helium isotope data

used in this study. Thus, since samples were collected at same location and time, S09 is based on exactly the same physical conditions (wind range, temperature range, etc) as experienced by the helium isotopes. We explored the consequence of using other gas exchange parameterizations that explicitly include bubbles, namely the Nicholson et al. (2011) (subsequently referred to as N11) parameterization and the Liang et al. (2013) parameterization (subsequently referred to as L13). N11 is based on a global inversion of deep N₂, Ar, N₂/Ar, and Kr/Ar data and thus reflects a larger perspective on gas exchange though perhaps one not quite as suitable to this specific study. N11 has a similar formulation for air injection to S09 although N11 does not include the effect of the partial pressure difference between enhanced pressure in the bubbles and pressure in the water when determining the flux due to partially trapped bubbles. L13 is based on a mechanistic model that explicitly includes the bubble size spectrum.

Calculations of the dynamic solubility equilibrium and the flux of ³He were also made using NCEP reanalysis winds instead of QuikSCAT winds. When NCEP reanalysis winds were used in the model, the gas exchange parameterization of Stanley et al. (2009b) was modified to a parameterization that was calculated using NCEP winds. For example, the gas exchange scaling factor, γ_G , is 0.97 when using QuikSCAT winds (as reported in (Stanley et al., 2009b) but is only 0.7 using NCEP winds.

The ³He flux, calculated from Eq. 1, is then corrected for the flux of ³He due to *in situ* tritium decay ($F_{\text{HeFromTrit}}$):

$$F_{\text{HeCorr}} = F_{\text{He}} - F_{\text{HeFromTrit}} \quad (7)$$

$F_{\text{HeFromTrit}}$ is calculated by using the radioactive decay equation ($A=N\lambda$ where A is activity of ³He, N = number of atoms of tritium and λ is half-life of tritium), the half-life of tritium ($\lambda=12.31$

years), and the mixed layer tritium concentrations measured concurrently with the ^3He data presented in this study. This yields a flux of ^3He produced in numbers of moles m^{-3} . We then multiply this flux by 300 m to calculate a flux in units of mol m^{-2} for the ^3He produced by tritium decay in upper 300 m of the ocean. This flux equals roughly 15% of the total ^3He flux calculated from Eq. 1 and is subtracted from the total ^3He flux to yield the ^3He flux that must be supported by vertical transport (Eq 7).

The nitrate flux (F_{NO_3}) was then calculated as the product between the corrected ^3He flux and the Nitrate: ^3He ratio (R):

$$F_{\text{NO}_3} = F_{\text{HeCorr}} \times R \quad (8)$$

The ratio R was calculated by determining the slope of a type II regression of NO_3 vs. ^3He for samples measured in the upper 400 m of water during the three year time series ($N=218$). Only data with $[\text{NO}_3] > 2 \text{ umol kg}^{-1}$ were used in the regression since water with NO_3 concentration below this threshold represents water in the euphotic zone where ^3He and NO_3 are decoupled. Jenkins and Doney (2003) studied the effect of using different data for the $\text{NO}_3/^3\text{He}$ correlation – data based on vertical correlation (as done here), on density surfaces, or at base of winter mixed layer, – and found the slopes were similar no matter which dataset was used.

3. Results and Discussion

3.1 The Fluxes of Helium-3 and Nitrate

The ^3He and tritium data collected in this study between 2003 and 2006 are presented in Fig. 1. The gradient of ^3He with depth is clearly visible. In contrast, tritium has a more uniform distribution with depth in the upper 300 m. The lack of excess ^3He in the mixed layer (mixed layer is demarcated by thick black line) is because of air-sea gas exchange, which results in a flux of excess ^3He out of the ocean into the atmosphere. This sustained air-sea gas exchange results in a decreasing inventory of tritiogenic ^3He in the ocean through time. Multiple measurements within the mixed layer were averaged in order to calculate the mixed layer concentrations of ^3He (Fig. 2a). The dynamic solubility equilibrium (blue curve on Fig. 2a) is significantly smaller than the ^3He concentrations, resulting in a sea to air flux of ^3He (Fig. 2c).

Additionally, since we now have a better understanding of the dynamic solubility equilibrium, both because of the extensive information on gas exchange garnered by the noble gases and because of more accurate estimates of molecular diffusivity of ^3He , we also have recalculated the ^3He and nitrate fluxes for the data from 1985-1988 that was originally presented in Jenkins and Doney (2003). Thus the ^3He concentrations from 1985-1988 as well as the dynamic solubility equilibrium for that time-period are presented in Fig 2b. Note the difference of scales in Fig. 2a and 2b. There is much less ^3He in 2003-2006 than in the 1980s because of a decreased ^3He source in the thermocline due to tritium decay over time and decades of outgassing of ^3He .

The average ^3He flux, corrected for tritium ingrowth, over the 2003-2006 time period is calculated to be $7.9 \pm 1 \text{ pmol m}^{-2} \text{ y}^{-1}$ (Table 1). The flux due to tritium ingrowth in the mixed layer, determined using the average tritium concentration and considering tritium that could be accessed in the upper 300 m of the ocean, during this period was $1.2 \pm 0.1 \text{ pmol m}^{-2} \text{ y}^{-1}$. The integrated ^3He flux is multiplied by a $\text{NO}_3: ^3\text{He}$ ratio of $82.9 \times 10^9 \pm 2 \times 10^9 \text{ mol NO}_3 / \text{mol } ^3\text{He}$

(Fig. 3) in order to calculate a NO_3 flux of $0.65 \pm 0.14 \text{ mol N m}^{-2} \text{ y}^{-1}$. The nitrate flux calculated by the flux gauge method used here represents the lower bound of new production in the northern half of the subtropical gyre. It represents a lower bound estimate because it only includes the new production based on the upward physical transport of nutrients. It does not include any new production due to nitrogen fixation, zooplankton migration, or atmospheric deposition of nitrate. At BATS, nitrogen fixation has been estimated to be 0.03 to $0.08 \text{ mol N m}^{-2} \text{ y}^{-1}$ (Singh et al., 2013;Knapp et al., 2008), which is equivalent to 5% to 12% of the new production we report from the flux gauge method. Zooplankton migration from 2003 to 2006 has been estimated to support a new production of $2 \text{ g C m}^{-2} \text{ y}^{-1}$ (Steinberg et al., 2012), which is equivalent to $0.025 \text{ mol N m}^{-2} \text{ y}^{-1}$ using the revised Redfield ratios of Anderson and Sarmiento (1994), and thus is only 4% of the new production rate estimated by the flux gauge technique. Estimates of the nitrate supply due to atmospheric deposition range from $0.006 \text{ mol N m}^{-2} \text{ y}^{-1}$ to $0.026 \text{ mol N m}^{-2} \text{ y}^{-1}$ (Singh et al., 2013;Knapp et al., 2010), thus being at most 4% of the new production flux estimated here from the flux gauge method. Thus in total, the sources of new nitrate that are not accounted by the flux gauge method may mean that the new production estimate given here is only about 80% to 85% of the total new production rate. The flux estimate represents the northern half of the gyre – rather than just the BATS site – because the water in the thermocline that is vertically transported at the BATS site sources from the Northern half of the gyre (Talley, 2003).

The nitrate fluxes calculated with the NCEP wind-derived ^3He fluxes are very similar to those calculated by QuikSCAT winds (Table 1). This is because the gas exchange parameterizations we used to calculate the flux from the ^3He concentration data and to calculate the dynamic solubility equilibrium were separately tuned to observed noble gas data for

QuikSCAT and NCEP. We were able to do this since we had the wealth of noble gas data collected concurrently allowing for a good model of air-sea gas exchange with two different wind products.

3.2 Uncertainties and Sensitivity Studies

There are a number of sources of uncertainty in the estimate of nitrate fluxes from the helium flux gauge technique. Here we describe these uncertainties and the results of sensitivity studies examining the effect of the sources of error. Table 2 lists the main sources of uncertainty in the calculations. One of the largest sources of uncertainty is uncertainty in the gas transfer velocity k (Eq. 1). Stanley et al. (2009b) illustrates how the time-series of noble gases collected concurrently with this data results in uncertainties of 14% in the gas transfer velocity k . Since k is directly used to calculate the ^3He air-sea flux from the difference between measured ^3He concentration and dynamic solubility equilibrium, this uncertainty directly translates to a 14% uncertainty in ^3He flux and ultimately in nitrate flux.

The second largest uncertainty in the nitrate flux is the uncertainty in the dynamic solubility equilibrium caused by uncertainties in parameterization of air injection. Three different parameterizations of air injection were used (see Section 2.2) in order to investigate the robustness of the flux gauge number with respect to air injection. The nitrate fluxes determined using these three different parameterizations when calculating the dynamic solubility equilibrium are $0.65 \text{ mol m}^{-2} \text{ y}^{-1}$ with S09, $0.55 \text{ mol m}^{-2} \text{ y}^{-1}$ with N11, and $0.48 \text{ mol m}^{-2} \text{ y}^{-1}$ with L13. The standard deviation of these three numbers ($0.08 \text{ mol m}^{-2} \text{ y}^{-1} = 13\%$ of reported nitrate flux) is used as a measure of the uncertainty due to air injection. The S09 value was used for reporting

1 the “base case” number (i.e. number reported in abstract and conclusion) because S09 is based on
2 data collected at same time and location as the ^3He data used in this study and thus is likely to
3 reflect gas exchange best in these conditions. Notably the root mean square deviation between
4 observed helium surface saturation anomalies and saturation anomalies predicted by the PWP
5 model run with either the S09 or N11 parameterization is the same (1.3%). The root mean square
6 deviation, however, for the model-data fit of the L13 parameterization is almost double that
7 (2.5%), suggesting that L13 is not representing air injection at this location and time as well as
8 S09 or N11. The root mean square deviation between model and data for surface saturation
9 anomalies for all the other stable noble gases (Ne, Ar, Kr and Xe) agree better for S09 and N11
10 than for L13 though the difference becomes smaller for the heavier gases – i.e. the L13 model
11 matches observed data almost as well for Kr or for Xe as does S09 or N11. Since the L13 model
12 does not match the surface saturation anomalies of He as well as S09 or N11 (i.e. double the
13 RMSD), L13 is probably not a good model to use for air injection in this study and thus
14 calculating the uncertainty from the standard deviation of fluxes determined when using all three
15 gas exchange parameterization is a conservative estimate of the total uncertainty due to air
16 injection. We also examined the effect on the nitrate flux of using different sets of air injection
17 parameters from the S09 parameterization. Specifically, we use many of the parameter sets
18 determined in Table 1 of Stanley et al. (2009b) including the sets of parameters determined for
19 different physical parameters in the model and different weightings of the cost function. We
20 found that the dynamic solubility equilibrium changed by only a small amount in these scenarios
21 so that the overall standard deviation of the ^3He flux for all the different scenarios of S09 was
22 only 2%.

1 The third largest source of uncertainty in the nitrate flux is the uncertainty in the
2 determination of dynamic solubility equilibrium due to uncertainties in the molecular diffusivity
3 of ^3He with respect to ^4He . The dynamic solubility equilibrium is sensitive to the molecular
4 diffusivity due to the relative diffusive gas exchange of ^3He vs. ^4He (i.e. Schmidt number
5 dependence) and due to the effect of air injection of partially trapped bubbles – during air
6 injection, ^3He diffuses more quickly out of the bubbles than ^4He . We ran sensitivity studies with
7 the range of molecular diffusivities estimated by Bourg and Sposito (2008) and found that the
8 ^3He flux changed by $\pm 10\%$ depending on the molecular diffusivities used. Although experiments
9 with helium isotopes have not yet been performed to confirm the diffusivities predicted by
10 Bourg and Sposito (2008) two separate experimental studies (Tempest and Emerson,
11 2013; Tyroller et al., 2014) have shown good agreement with the Ne isotope diffusivities
12 calculated by Bourg and Sposito (2008), giving us confidence in the Bourg and Sposito (2008)
13 helium predictions.

14 The effect of measurement error of ^3He is a smaller uncertainty than the systematic
15 uncertainties listed above but does lead to an error of 5% when propagated through all the
16 calculations. Interestingly, for the 1985-1988 period, the absolute ^3He concentrations were much
17 higher but the measurement uncertainty at that time was much worse, resulting in a similar 5%
18 contribution of measurement uncertainty during that period as well.

19 Uncertainties in the slope of $\text{NO}_3\text{:}^3\text{He}$ feed directly into uncertainty in the nitrate flux,
20 resulting in a 2.5% uncertainty in the nitrate flux. The uncertainties were derived from the
21 uncertainty associated with the calculation of the slope using a type II regression and appropriate
22 measurement uncertainties for the individual data points. Additional error in the ^3He flux – and
23 thus propagated to the nitrate flux – comes from the correction for tritium ingrowth in the water

column. However, since the ^3He flux due to *in situ* tritium production is relatively small (12% of the total ^3He flux), the uncertainty on that number only contributes to a small fraction of the total uncertainty in the helium and nitrate fluxes (1%).

3.3 Comparison to 1980s Fluxes

The estimated nitrate flux for the period between 1985 to 1988 is 50% larger than the nitrate flux for the 2003-2006 period, though over half of this difference can be accounted for by uncertainties in the flux estimates. For 1985-1988, our recomputed nitrate flux estimate is $1.05 \pm 0.2 \text{ mol N m}^{-2} \text{ y}^{-1}$ (Table 1), which is 25% larger than the nitrate flux calculated for the same time period in Jenkins and Doney (2003). This difference between the 1985-1988 fluxes calculated here versus those calculated in Jenkins and Doney (2003) stems from this calculation using a well-modeled dynamic solubility equilibrium. In the earlier study, we did not have the other noble gas data nor updated estimates of molecular diffusivity (Bourg and Sposito, 2008) and thus employed a simpler and likely less accurate estimate of the dynamic solubility equilibrium.

It is interesting to note that although the nitrate flux in 1985-1988 is only 50% larger than the nitrate flux in 2003-2006, the ^3He flux in 1985-1988 is 300% larger than the ^3He flux in 2003-2006. This is because in the 1980s, there was a much larger tritium inventory and consequently larger concentrations of ^3He in the main thermocline (Fig. 4). However, the slope of the $\text{NO}_3\text{:}^3\text{He}$ relationship also changes with time. The distribution of nutrients in the main thermocline are in an approximate steady state established by a balance between nutrient release by *in situ* remineralization of organic material and removal by physical processes related to

1 ventilation, advection, and mixing. The corresponding thermocline distribution of tritiogenic ^3He
2 is evolving as a transient tracer. Over time, as the bomb-tritium pulse penetrates the thermocline,
3 the resultant ^3He maximum deepens and broadens [Jenkins, 1998]. Consequently the relationship
4 between ^3He and nutrients is changing with time. Figure 3 is a plot of the $\text{NO}_3\text{:}^3\text{He}$ relationship
5 for the upper 500 m of the water column near Bermuda at four points in time. Notably, the slope
6 of the $\text{NO}_3\text{:}^3\text{He}$ relationship has increased by over a factor of two in the approximately 25 years
7 spanned by this data.

8 While the nitrate flux is broadly similar between the two time periods, there is still a 50%
9 difference with the flux being larger in 1985-1988 than in 2003-2006. What can account for this
10 difference? It is not because of NCEP winds being used in the 1985-1988 calculation and
11 QuikSCAT winds being used in the 2003-2006 calculation, because even if we do the 2003-2006
12 calculation with NCEP winds, we still get a 40% difference between the flux in the two different
13 decades (Table 1). It also is not likely due to the 1985-1988 data being from Hydrostation S
14 whereas the 2003-2006 data is from BATS. Those two sites are only 28 km apart and since the
15 ^3He flux gauge estimate is reflection of a much broader region, the relatively small difference in
16 locations of samples likely does not play a role. It could be, in part, due to a time lag between the
17 evolving subsurface $\text{NO}_3\text{-}^3\text{He}$ ratio and surface fluxes. Most likely, however, it is due to a real
18 elevation in new production in the late 1980s compared to the 2003-2006 period. Winter mixed
19 layers in the two time periods are similar, with the exception of a shallower than typical winter
20 mixed layer depth in 1986, and thus are likely not an explanation for the difference in production
21 between the periods.

22 Lomas et al. (2010) observed significant changes in export production at BATS over
23 time, with the period between 1988 and 1995 having lower export fluxes than the period from

1 1995 to 2008. They attributed these changes to a shift in the North Atlantic Oscillation (NAO)
2 from positive in the 1988 to 1995 period to neutral in the 1996 to 2008 period. Our older data is
3 from 1985 to 1988 and was not included in the Lomas et al. (2010) study. The winter NAO index
4 (JFM) which has been shown to be most sensitive to changes in subtropical mode water
5 formation (Billheimer and Talley, 2013) and primary production (Lomas et al., 2010) was -1.2,
6 0.2, and -1.1 for 1985, 1986 and 1987 respectively. It was -0.3, -0.5, and -0.6 for 2004, 2005, and
7 2006 respectively. A more negative winter NAO, as was mostly seen in 1985-1988 period,
8 according to Lomas et al. (2010) would be associated with higher production, which is indeed
9 what we found in this study.

10 A more negative NAO is usually correlated with a greater production of subtropical mode
11 waters (STMW) via enhanced surface buoyancy loss and vertical convection (Billheimer and
12 Talley, 2013). Indeed, estimates of Kelly and Dong (2013) suggest that there was increased
13 formation of STMW in 1985-1988 compared to 2003-2006. We thus find higher rates of new
14 production are associated with time periods of higher generation of STMW. This is in contrast to
15 the hypothesis of Palter et al. (2005) who suggested that increased STMW production would lead
16 to a reduction in primary production due to decreased nutrients below the mixed layer in the
17 vertically-homogenized mode water region since the decreased nutrients would lead to a smaller
18 nutrient supply from the main thermocline below the mode water region and thus to smaller rates
19 of primary production.

20 The highest annual flux in the 1985-1988 period comes from 1987 (Fig. 2d).
21 Interestingly, while the NAO index of 1987 was similar to that of 1985 and 2003-2006, the NAO
22 index of 1986 was positive. It has been shown that chlorophyll correlates better with NAO index
23 at BATS using a one year time lag (Cianca et al., 2012). Thus potentially the higher fluxes we

see in 1987 are a result of the higher NAO index in 1986. However, this would be counter to the general trend suggested by Lomas et al. (2010) and seen in the rest of our data of higher rates of production with more negative NAO indices.

3.4 Seasonal Cycle

A seasonal cycle in ^3He flux is observed in both the 1985-1988 time period and the 2003-2006 time period (Fig. 5). The ^3He fluxes are highest in winter-time when the deep winter mixed layers at BATS mine water from the seasonal thermocline, bringing up higher amounts of ^3He and nitrate. But even in the summer, there is an upward flux of ^3He suggesting an upward flux of nitrate. There is no observable nitrate in the summer mixed layer at BATS (Michaels et al., 1994; Steinberg et al., 2001) likely because the organisms consume all the nitrate as soon as it enters the euphotic zone. Thus the lack of observable nitrate, long known at BATS, does not mean that nitrate was never there. Hence the “paradox” of how summertime production can be supported at BATS without observable nutrients is in some sense answered by this clear sign that there is an upward nutrient flux, even in the summer. This supports the recent finding of Fawcett et al. (2014) showing evidence of nitrate supply to the mixed layer at BATS even in the summer.

3.5 Comparison to other rates of biological productivity at BATS

The rate of new production estimated by the helium flux gauge technique presented in this study is larger than most of the rates of new production, net community production or export production at BATS derived from other geochemical tracer approaches. Over long periods of time and long spatial scales, new production, net community production and export production

1 should be equal (Dugdale and Goering, 1967). In carbon units, using the revised Redfield ratio of
2 Anderson and Sarmiento (1994) of 106:16, new production estimated in this study was 4.3 ± 0.9
3 $\text{mol C m}^{-2} \text{ y}^{-1}$ in 2003-2006 and $6.96 \pm 1.3 \text{ mol C m}^{-2} \text{ y}^{-1}$ in 1985-1988. Because of global and
4 regional variations in the C:N ratio (Lomas et al., 2013; Martiny et al., 2013; Ono et al., 2001),
5 there are additional uncertainties when converting nitrate fluxes to carbon fluxes. Additionally,
6 as noted above, these rates represent new production derived from physical vertical supply of
7 nitrate over the Northern half of the subtropical gyre.

8 Export fluxes as estimated by apparent oxygen utilization rates (AOUR) also represent fluxes
9 over a similar northern region (Jenkins, 1980). Tritium samples were collected and used in
10 conjunction with ^3He and O_2 data from the same cruises in 2003-2006 that the ^3He data in this
11 paper come from to estimate apparent oxygen utilization rates (Stanley et al., 2012). The AOURL
12 values were integrated to 500 m to yield a lower bound on annual export from the
13 remineralization and oxygen consumption between 200 m and 500 m of $2.1 \pm 0.5 \text{ mol C m}^{-2} \text{ y}^{-1}$.
14 Thus the fluxes estimated by the helium flux gauge technique are nearly a factor of two greater
15 than the fluxes by AOURL, even though both represent a large geographical region.

16 A more local estimate of production comes from seasonal drawdown of DIC at BATS or by
17 seasonal accumulation of O_2 with respect to Ar. Both techniques rely on the fact that
18 photosynthesis produces O_2 and consumes CO_2 whereas respiration produces CO_2 and consumes
19 O_2 . Thus the seasonal changes in O_2 or CO_2 constrain the net balance between photosynthesis
20 and respiration. On the same cruises as data for ^3He flux gauge technique were collected, the
21 seasonal accumulation of O_2 and Ar was measured and used to estimate rates of net community
22 production of 1.2 to $2.4 \text{ mol C m}^{-2} \text{ y}^{-1}$ (Stanley, 2007). Notably, this rate is similar to that of the
23 AOURL estimate and a factor of 2 smaller than the ^3He flux gauge estimate. The seasonal

1 accumulation of oxygen and argon has been used at other time periods to estimate the rate of net
2 community production at BATS to be 2.2 to 3 mol C m⁻² y⁻¹ (Spitzer and Jenkins, 1989; Luz and
3 Barkan, 2009). Seasonal drawdown of DIC directly as well as the change in isotopic composition
4 of ¹³C of DIC have been used to estimate annual net community production fluxes of 1.7 to 4.9
5 mol C m⁻² y⁻¹ (Gruber et al., 1998; Brix et al., 2006; Fernandez-Castro et al., 2012). The upper end
6 of this range approximates the rate of new production we find here using the flux gauge
7 technique. Interestingly, the DIC drawdown and O₂/Ar approaches reflect a smaller spatial scale
8 than the AOOR estimates, but at least in some cases agree better with the ³He flux gauge
9 approach.

10 On even smaller spatial and temporal scales, ²³⁴Th has been used to estimate export
11 fluxes at BATS, resulting in rates of export production calculated to be 0.3 to 0.8 mol C m⁻² y⁻¹
12 (Maiti et al., 2009) These fluxes are much smaller than the fluxes estimated by other
13 geochemical tracers, which may in part be due to the fact that the ²³⁴Th technique does not
14 include the contribution of export due to DOC whereas the other geochemical techniques do.
15 DOC export in the Sargasso Sea has been estimated to be up to 1 mol C m⁻² y⁻¹ (Hansell et al.,
16 2012).

17 Why is the helium flux gauge technique yielding rates of new production at the high end
18 of the range of rates from other geochemical tracers? In part this may be due to the broader
19 spatial coverage of the flux gauge technique, but that is not enough to explain fully the
20 discrepancy since the AOOR technique has similar spatial area but smaller fluxes. One reason
21 may be that ³He and NO₃ are decoupled during obduction in the northern part of the gyre. The
22 northwest Sargasso Sea, where the warm waters of the Gulf Stream leave the North American
23 continent, is characterized by large latent heat fluxes and substantial downstream winter mixed

layer deepening (Worthington, 1972). In effect, upper thermocline isopycnals outcrop, a process referred to as obduction (Qiu and Huang, 1995). This outcropping brings remineralized nutrients and tritiogenic ^3He back to the seasonal layer. Whereas the time constant associated with nutrient removal by biological processes is a matter of days, the exchange time-scale for tritiogenic ^3He loss to the atmosphere from a deep mixed layer may be several weeks. In this respect the nutrients may have been removed while the ^3He “signal” may persist, so the ^3He flux gauge may measure not only local new production, but may also hold a more “regional” memory of the upstream, previous winter’s production.

There are two approaches to estimating this obduction flux of ^3He (and hence via the flux gauge, NO_3). Given that they are rather crude in nature, and involve rather different assumptions and more importantly scale, exact congruence would be unlikely. All that one can ask is if they are broadly compatible with accommodating the fluxes obtained in this study. One way is to compute the eastward transport of ^3He through 52°W in the upper 300 m. Using the 2003 CLIVAR A20 section and geostrophic velocities relative to 200 decibars (data are publicly available from <http://cchdo.ucsd.edu>) (Jenkins and Stanley, 2008), the peak transport south of 38°N is $1.4 \mu\text{mol s}^{-1}$. When this transport is averaged over the area of the northern half of the Sargasso Sea (approximately $3 \times 10^6 \text{ km}^2$), this corresponds to a flux of $\sim 0.5 \text{ amol m}^{-2}\text{s}^{-1}$, or $\sim 15 \text{ pmol m}^{-2}\text{y}^{-1}$ in 2003. The second calculation is based on the work of Qiu and Huang (1995) who estimated an obduction rate ranging from 50 to 250 m y^{-1} in the northern Sargasso Sea (their figure 7f). Typical excess ^3He concentrations range from 0.02 to 0.04 pmol m^{-3} at 300 m depth, so one infers an upward ^3He flux ranging from 1 to $10 \text{ pmol m}^{-2} \text{ y}^{-1}$. The ^3He flux determined in this study is $7.9 \text{ pmol m}^{-2} \text{ y}^{-1}$ and thus fits within the range of estimates of flux due to obduction.

4. Conclusions

1 In summary, we have used the approach of Jenkins and Doney (Jenkins and Doney, 2003) to
2 calculate the *physical* supply of subsurface nitrate to the euphotic zone at BATS to be $0.65 \pm$
3 $0.14 \text{ mol m}^{-2} \text{ y}^{-1}$. This flux may support the new production of approximately $4.3 \pm 0.9 \text{ mol C m}^{-2}$
4 y^{-1} due to the upward flux of nutrients over a broad region of the subtropical Northwestern
5 Atlantic. This reflects a lower bound on total new production since nitrate may come from other
6 sources as well (nitrogen fixation, vertical migration, etc) and thus may be underestimating total
7 new production by 15%. We show that the rates are consistent with, but lower than, rates of new
8 production recalculated from similar data from 1985-1988 and that this difference may be related
9 to subtropical mode water formation. We also show that the rates estimated by this technique are
10 higher than most other rates of new production estimated at the BATS site. This work thus shows
11 that upward flux of nutrients – even if not directly observed at BATS by traditional techniques –
12 is more than sufficient to support the observed rates of net community production and export
13 production calculated at BATS.

16 **5. Acknowledgements**

17 We would like to thank Mike Lomas, Rod Johnson, and the BATS research team for the
18 opportunity to collect samples. We would like to thank Steven Emerson and one anonymous
19 reviewer for their helpful suggestions. We are grateful for the assistance of the captain and crew
20 of the R/V Weatherbird II and the R/V Atlantic Explorer. This research was funded by the
21 National Science Foundation (OCE-1434000 and OCE-221247).

6. References

- Anderson, L. A., and Sarmiento, J. L.: Redfield ratios of remineralization determined by nutrient data-analysis, *Global Biogeochemical Cycles*, 8, 65-80, 1994.
- Benson, B. B., and Krause, D., Jr.: Isotopic fractionation of helium during solution: a probe for the liquid state, *Journal of Solution Chemistry*, 9, 895-909, 1980.
- Billheimer, S., and Talley, L. D.: Near cessation of Eighteen Degree Water renewal in the western North Atlantic in the warm winter of 2011-2012, *J. Geophys. Res.-Oceans*, 118, 6838-6853, 10.1002/2013jc009024, 2013.
- Bourg, I. C., and Sposito, G.: Isotopic fractionation of noble gases by diffusion in liquid water: Molecular dynamics simulations and hydrologic applications, *Geochimica Et Cosmochimica Acta*, 72, 2237-2247, 2008.
- Brew, H. S., Moran, S. B., Lomas, M. W., and Burd, A. B.: Plankton community composition, organic carbon and thorium-234 particle size distributions, and particle export in the Sargasso Sea, *Journal of Marine Research*, 67, 845-868, 2009.
- Brix, H., Gruber, N., Karl, D. M., and Bates, N. R.: On the relationships between primary, net community, and export production in subtropical gyres, *Deep-Sea Research Part II-Topical Studies in Oceanography*, 53, 698-717, 2006.
- Broecker, W. S., and Peng, T. H.: The distribution of bomb-produced tritium and radiocarbon at GEOSECS station 347 in the eastern North Pacific, *Earth and Planetary Science Letters*, 49, 453-462, 1980.
- Buesseler, K. O.: Do upper-ocean sediment traps provide an accurate record of particle flux?, *Nature*, 353, 420-423, 1991.
- Buesseler, K. O., Lamborg, C., Cai, P., Escoube, R., Johnson, R., Pike, S., Masque, P., McGillicuddy, D., and Verdeny, E.: Particle fluxes associated with mesoscale eddies in the Sargasso Sea, *Deep-Sea Research Part II-Topical Studies in Oceanography*, 55, 1426-1444, 10.1016/j.dsr2.2008.02.007, 2008.
- Cianca, A., Godoy, J. M., Martin, J. M., Perez-Marrero, J., Rueda, M. J., Llinas, O., and Neuer, S.: Interannual variability of chlorophyll and the influence of low-frequency climate modes in the North Atlantic subtropical gyre, *Global Biogeochemical Cycles*, 26, Gb2002/10.1029/2010gb004022, 2012.
- Doney, S. C., Glover, D. M., and Jenkins, W. J.: A model function of the global bomb-tritium distribution in precipitation, 1960-1986, *Journal of Geophysical Research*, 97, 5481-5492, 1992.
- Dong, S. F., and Kelly, K. A.: How Well Do Climate Models Reproduce North Atlantic Subtropical Mode Water?, *J. Phys. Oceanogr.*, 43, 2230-2244, 10.1175/jpo-d-12-0215.1, 2013.
- Dugdale, R. C., and Goering, J. J.: Uptake of new and regenerated forms of nitrogen in primary productivity., *Limnology and Oceanography*, 12, 196-206, 1967.
- Dugdale, R. C., Wilkerson, F. P., Barber, R. T., and Chavez, F. P.: Estimating new production in the equatorial Pacific Ocean at 150W, *Journal of Geophysical Research*, 97, 681-686, 1992.
- Fawcett, S. E., Lomas, M. W., Ward, B. B., and Sigman, D. M.: The counterintuitive effect of summer-to-fall mixed layer deepening on eukaryotic new production in the Sargasso Sea, *Global Biogeochemical Cycles*, 28, 86-102, 10.1002/2013gb004579, 2014.
- Fernandez-Castro, B., Anderson, L., Maranon, E., Neuer, S., Ausin, B., Gonzalez-Davila, M., Santana-Casiano, M., Cianca, A., Santana, R., Llinas, O., Rueda, M. J., and Mourino-Carballido, B.: Regional differences in modelled net production and shallow remineralization in the North Atlantic subtropical gyre, *Biogeosciences*, 9, 2831-2846, 10.5194/bg-9-2831-2012, 2012.
- Fuchs, G., Roether, W., and Schlosser, P.: Excess ^3He in the ocean surface layer, *Journal of Geophysical Research*, 92, 6559-6568, 1987.

- 1 Graham, A., Woolf, D. K., and Hall, A. J.: Aeration due to breaking waves. Part I: Bubble populations, J.
- 2 Phys. Oceanogr., 34, 989-1007, 2004.
- 3 Gruber, N., Keeling, C. D., and Stocker, T. F.: Carbon-13 constraints on the seasonal inorganic carbon
- 4 budget at the BATS site in the northwestern Sargasso Sea, Deep-Sea Research Part I, 45, 673-717,
- 5 1998.
- 6 Hansell, D. A., Carlson, C. A., and Schlitzer, R.: Net removal of major marine dissolved organic carbon
- 7 fractions in the subsurface ocean, Global Biogeochemical Cycles, 26,
- 8 Gb1016.10.1029/2011gb004069, 2012.
- 9 Harrison, W. G., and Harris, L. R.: Isotope-Dilution and Its Effects on Measurements of Nitrogen and
- 10 Phosphorus Uptake by Oceanic Microplankton, Marine Ecology-Progress Series, 27, 253-261,
- 11 1986.
- 12 Jahne, B., Heinz, G., and Dietrich, W.: Measurement of the diffusion coefficients of sparingly soluble
- 13 gases in water, Journal of Geophysical Research, 92, 10767-10776, 1987.
- 14 Jenkins, W. J.: Tritium and He-3 in the Sargasso Sea, Journal of Marine Research, 38, 533-569, 1980.
- 15 Jenkins, W. J., and Goldman, J. C.: Seasonal oxygen cycling and primary production in the Sargasso Sea,
- 16 Journal of Marine Research, 43, 465-491, 1985.
- 17 Jenkins, W. J.: Nitrate flux into the euphotic zone near Bermuda, Nature, 331, 521-523, 1988a.
- 18 Jenkins, W. J.: Nitrate flux into the euphotic zone near Bermuda, Nature, 331, 521-523, 1988b.
- 19 Jenkins, W. J.: The use of anthropogenic tritium and ³He to study subtropical gyre ventilation and
- 20 circulation, Philosophical Transactions of the Royal Society (London), A325, 43-61, 1988c.
- 21 Jenkins, W. J., and Doney, S. C.: The subtropical nutrient spiral, Global Biogeochemical Cycles, 17, 1110,
- 22 doi:1110.1029/2003GB002085, 2003.
- 23 Jenkins, W. J., and Stanley, R. H. R.: The Helium-3 flux gauge in the subtropical North Atlantic: What does
- 24 it tell us about nutrient fluxes and new production in an oligotrophic gyre?, Ocean Sciences
- 25 Meeting, Orlando, FL, 2008.
- 26 Kalnay, E., Kanamitsu, M., Kistler, R., Collins, W., Deaven, D., Gandin, L., Iredell, M., Saha, S., White, G.,
- 27 Woollen, J., Zhu, Y., Chelliah, M., Ebisuzaki, W., Higgins, W., Janowiak, J., Mo, K. C., Ropelewski,
- 28 C., Wang, J., Leetmaa, A., Reynolds, R., Jenne, R., and Joseph, D.: The NCEP/NCAR 40-year
- 29 reanalysis project, Bulletin of the American Meteorological Society, 77, 437-471, 1996.
- 30 Knapp, A. N., DiFiore, P. J., Deutsch, C., Sigman, D. M., and Lipschultz, F.: Nitrate isotopic composition
- 31 between Bermuda and Puerto Rico: Implications for N(2) fixation in the Atlantic Ocean, Global
- 32 Biogeochemical Cycles, 22, Gb3014.10.1029/2007gb003107, 2008.
- 33 Knapp, A. N., Hastings, M. G., Sigman, D. M., Lipschultz, F., and Galloway, J. N.: The flux and isotopic
- 34 composition of reduced and total nitrogen in Bermuda rain, Marine Chemistry, 120, 83-89,
- 35 10.1016/j.marchem.2008.08.007, 2010.
- 36 Liang, J. H., Deutsch, C., McWilliams, J. C., Baschek, B., Sullivan, P. P., and Chiba, D.: Parameterizing
- 37 bubble-mediated air-sea gas exchange and its effect on ocean ventilation, Global Biogeochemical
- 38 Cycles, 27, 894-905, 10.1002/gbc.20080, 2013.
- 39 Lipschultz, F.: A time-series assessment of the nitrogen cycle at BATS, Deep-Sea Research Part II-Topical
- 40 Studies in Oceanography, 48, 1897-1924, 10.1016/s0967-0645(00)00168-5, 2001.
- 41 Lipschultz, F., Bates, N. R., Carlson, C. A., and Hansell, D. A.: New production in the Sargasso Sea: History
- 42 and current status, Global Biogeochemical Cycles, 16, 1001.10.1029/2000gb001319, 2002.
- 43 Lomas, M. W., Steinberg, D. K., Dickey, T., Carlson, C. A., Nelson, N. B., Condon, R. H., and Bates, N. R.:
- 44 Increased ocean carbon export in the Sargasso Sea linked to climate variability is countered by its
- 45 enhanced mesopelagic attenuation, Biogeosciences, 7, 57-70, 2010.
- 46 Lomas, M. W., Bates, N. R., Johnson, R. J., Knap, A. H., Steinberg, D. K., and Carlson, C. A.: Two decades
- 47 and counting: 24-years of sustained open ocean biogeochemical measurements in the Sargasso

1 Sea, Deep-Sea Research Part II-Topical Studies in Oceanography, 93, 16-32,
2 10.1016/j.dsr.2013.01.008, 2013.

3 Lott, D. E., and Jenkins, W. J.: Advances in analysis and shipboard processing of tritium and helium
4 samples, International WOCE Newsletter, 30, 27-30, 1998.

5 Luz, B., and Barkan, E.: Net and gross oxygen production from O-2/Ar, O-17/O-16 and O-18/O-16 ratios,
6 Aquatic Microbial Ecology, 56, 133-145, 2009.

7 MacMahon, D.: Half-life evaluations for ^3H , ^{90}Sr , and ^{90}Y , Applied Radiation and Isotopes, 54, 1417-1419,
8 2006.

9 Maiti, K., Benitez-Nelson, C. R., Lomas, M. W., and Krause, J. W.: Biogeochemical responses to late-
10 winter storms in the Sargasso Sea, III-Estimates of export production using Th-234:U-238
11 disequilibria and sediment traps, Deep-Sea Res. Part I-Oceanogr. Res. Pap., 56, 875-891,
12 10.1016/j.dsr.2009.01.008, 2009.

13 Maiti, K., Buesseler, K. O., Pike, S. M., Benitez-Nelson, C., Cai, P. H., Chen, W. F., Cochran, K., Dai, M. H.,
14 Dehairs, F., Gasser, B., Kelly, R. P., Masque, P., Miller, L. A., Miquel, J. C., Moran, S. B., Morris, P.
15 J., Peine, F., Planchon, F., Renfro, A. A., van der Loeff, M. R., Santschi, P. H., Turnewitsch, R.,
16 Waples, J. T., and Xu, C.: Intercalibration studies of short-lived thorium-234 in the water column
17 and marine particles, Limnol. Oceanogr. Meth., 10, 631-644, 10.4319/lom.2012.10.631, 2012.

18 Marra, J.: Approaches to the measurement of plankton production, Phytoplankton Productivity: Carbon
19 Assimilation in Marine and Freshwater Ecosystems, edited by: Williams, P. J. L., Thomas, D. N.,
20 and Reynolds, C. S., Blackwell, Malden, MA, 31 pp., 2002.

21 Marra, J.: Net and gross productivity: weighing in with C-14, Aquatic Microbial Ecology, 56, 123-131,
22 2009.

23 Martiny, A. C., Vrugt, J. A., Primeau, F. W., and Lomas, M. W.: Regional variation in the particulate
24 organic carbon to nitrogen ratio in the surface ocean, Global Biogeochemical Cycles, 27, 723-731,
25 10.1002/gbc.20061, 2013.

26 Michaels, A. F., Bates, N. R., Buesseler, K. O., Carlson, C. A., and Knap, A. H.: Carbon system imbalances
27 in the Sargasso Sea, Nature, 372, 537-540, 1994.

28 Ono, S., Ennyu, A., Najjar, R. G., and Bates, N. R.: Shallow remineralization in the Sargasso Sea estimated
29 from seasonal variations in oxygen, dissolved inorganic carbon and nitrate, Deep-Sea Research,
30 48, 1567-1582, 2001.

31 Ostlund, H. G., Dorsey, H. G., and Rooth, C. G.: GEOSECS North Atlantic Radiocarbon and Tritium Results,
32 Earth and Planetary Science Letters, 23, 69-86, 1974.

33 Owens, S. A., Buesseler, K. O., Lamborg, C. H., Valdes, J., Lomas, M. W., Johnson, R. J., Steinberg, D. K.,
34 and Siegel, D. A.: A new time series of particle export from neutrally buoyant sediments traps at
35 the Bermuda Atlantic Time-series Study site, Deep-Sea Res. Part I-Oceanogr. Res. Pap., 72, 34-47,
36 10.1016/j.dsr.2012.10.011, 2013.

37 Palter, J. B., Lozier, M. S., and Barber, R. T.: The effect of advection on the nutrient reservoir in the North
38 Atlantic subtropical gyre, Nature, 437, 687-692, 2005.

39 Peterson, B. J.: Aquatic Primary Productivity and the C-14-Co2 Method - a History of the Productivity
40 Problem, Annu. Rev. Ecol. Syst., 11, 359-385, 1980.

41 Price, J. F., Weller, R. A., and Pinkel, R.: Diurnal cycling - observations and models of the upper ocean
42 response to diurnal heating, cooling, and wind mixing, J. Geophys. Res.-Oceans, 91, 8411-8427,
43 1986.

44 Qiu, B., and Huang, R. X.: Ventilation of the North Atlantic and North Pacific: subduction versus
45 obduction, J. Phys. Oceanogr., 25, 2374-2390, 1995.

46 Rooth, C. G., and Ostlund, H. G.: Penetration of tritium into the North Atlantic thermocline, Deep-Sea
47 Research, 19, 481-492, 1972.

- 1 Scarratt, M. G., Marchetti, A., Hale, M. S., Rivkin, R. B., Michaud, S., Matthews, P., Levasseur, M., Sherry,
2 N., Merzouk, A., Li, W. K. W., and Kiyosawa, H.: Assessing microbial responses to iron enrichment
3 in the Subarctic Northeast Pacific: Do microcosms reproduce the in situ condition?, *Deep-Sea*
4 *Research Part II-Topical Studies in Oceanography*, 53, 2182-2200, 2006.
- 5 Singh, A., Lomas, M. W., and Bates, N. R.: Revisiting N₂ fixation in the North Atlantic Ocean: Significance
6 of deviations from the Redfield Ratio, atmospheric deposition and climate variability, *Deep-Sea*
7 *Research Part II-Topical Studies in Oceanography*, 93, 148-158, 10.1016/j.dsr2.2013.04.008, 2013.
- 8 Spitzer, W. S., and Jenkins, W. J.: Rates of vertical mixing, gas-exchange and new production - estimates
9 from seasonal gas cycles in the upper ocean near Bermuda, *Journal of Marine Research*, 47, 169-
10 196, 1989.
- 11 Stanley, R. H. R., Jenkins, W. J., and Doney, S. C.: Quantifying seasonal air-sea gas exchange processes
12 using noble gas time-series: A design experiment, *Journal of Marine Research*, 64, 267-295, 2006.
- 13 Stanley, R. H. R., Baschek, B., Lott, D. E., and Jenkins, W. J.: A new automated method for measuring
14 noble gases and their isotopic ratios in water samples, *Geochemistry Geophysics Geosystems*, 10,
15 doi:10.1029/2009GC002429, 2009a.
- 16 Stanley, R. H. R., Jenkins, W. J., Doney, S. C., and Lott III, D. E.: Noble Gas Constraints on Air-Sea Gas
17 Exchange and Bubble Fluxes, *Journal of Geophysical Research - Oceans*, 114,
18 doi:10.1029/2009JC005396, 2009b.
- 19 Stanley, R. H. R., Doney, S. C., Jenkins, W. J., and Lott III, D. E.: Apparent oxygen utilization rates
20 calculated from tritium and helium-3 profiles at the Bermuda Atlantic Time-series Study site,
21 *Biogeosciences*, doi:10.5194/bg-9-1969-2012, 9977-10015, 2012.
- 22 Stark, S., Jenkins, W. J., and Doney, S. C.: Deposition and recirculation of tritium in the North Pacific
23 Ocean, *Journal of Geophysical Research*, 109, doi:10.1029/2003JC002150,
24 doi:10.1029/2003JC002150, 2004.
- 25 Steinberg, D. K., Carlson, C. A., Bates, N. R., Johnson, R. J., Michaels, A. F., and Knap, A. H.: Overview of
26 the US JGOFS Bermuda Atlantic Time-series Study (BATS): a decade-scale look at ocean biology
27 and biogeochemistry, *Deep-Sea Research Part II-Topical Studies in Oceanography*, 48, 1405-1447,
28 10.1016/S0967-0645(00)00148-X, 2001.
- 29 Steinberg, D. K., Lomas, M. W., and Cope, J. S.: Long-term increase in mesozooplankton biomass in the
30 Sargasso Sea: Linkage to climate and implications for food web dynamics and biogeochemical
31 cycling, *Global Biogeochemical Cycles*, 26, Gb1004.10.1029/2010gb004026, 2012.
- 32 Stewart, G., Moran, S. B., Lomas, M. W., and Kelly, R. P.: Direct comparison of Po-210, Th-234 and POC
33 particle-size distributions and export fluxes at the Bermuda Atlantic Time-series Study (BATS) site,
34 *Journal of Environmental Radioactivity*, 102, 479-489, 10.1016/j.jenvrad.2010.09.011, 2011.
- 35 Talley, L. D.: Shallow, intermediate, and deep overturning components of the global heat budget, *J.*
36 *Phys. Oceanogr.*, 33, 530-560, 10.1175/1520-0485(2003)033<0530:siadoc>2.0.co;2, 2003.
- 37 Tempest, K. E., and Emerson, S.: Kinetic isotopic fractionation of argon and neon during air-water gas
38 transfer, *Marine Chemistry*, 153, 39-47, 10.1016/j.marchem.2013.04.002, 2013.
- 39 Tyroller, L., Brennwald, M. S., Maechler, L., Livingstone, D. M., and Kipfer, R.: Fractionation of Ne and Ar
40 isotopes by molecular diffusion in water, *Geochimica Et Cosmochimica Acta*, 136, 60-66,
41 10.1016/j.gca.2014.03.040, 2014.
- 42 Weiss, W. M., and Roether, W.: The rates of tritium input to the world oceans, *Earth and Planetary*
43 *Science Letters*, 49, 435-446, 1980.
- 44 Worthington, L. V.: Negative oceanic heat flux as a cause of watermass formation, *J. Phys. Oceanogr.*, 2,
45 205-211, 1972.

7. Figure Captions

Fig. 1. A time series of helium isotope ratio anomaly (in percent) relative to the atmospheric $^3\text{He}/^4\text{He}$ ratio (upper panel) and tritium (in Tritium Units) decay corrected to January, 2005 (lower panel) at the Bermuda Atlantic Time Series Site in the North Atlantic near Bermuda. Sampling, designated by black dots, was approximately monthly over the ~3 year period. The black line is the mixed layer depth estimated from the CTD data.

Fig. 2. Mixed layer $\delta^3\text{He}$ data from (a) 2003-2006 and (b) 1985-1988 as well as the dynamic solubility equilibrium for $\delta^3\text{He}$. Error bars represent standard error of multiple measurements within the mixed layer. Fluxes of ^3He calculated from the data for (c) 2003-2006 and (d) 1985-1988. Note the difference in scales on the y-axes for the two time periods.

Fig. 3. The observed relationship between excess (tritiogenic) ^3He and dissolved inorganic nitrate near Bermuda at four points in time. The 1986 and 2005 relations are based on approximately 3 year time series occupations near Bermuda (the former at Hydrostation S and the latter at BATS). The 1981 and 1997 data sets are from cruise stations within ~500 km of the site. Only samples with potential density anomalies less than 26.8 kg m^{-3} are plotted and used. Note the “water fall” effect at low ^3He and nitrate concentrations in the euphotic zone, where the two tracers become uncoupled due to differing boundary conditions. The straight lines, from which the slopes are obtained, are type II linear regressions (since there are errors associated with both ^3He and NO_3 a type II regression is appropriate) of points with nitrate concentrations in

1 excess of $2 \mu\text{mol kg}^{-1}$. The lower bound nitrate limit was chosen to avoid the tracer-decoupled
2 points.

3
4
5 Fig. 4. Representative profiles of $\delta^3\text{He}$ in the upper 1200 m of the water column in 1986 (blue)
6 and 2003-2006 (green). The profiles illustrate that in 1986 there was much higher $\delta^3\text{He}$ in the
7 main thermocline and a larger gradient between the thermocline and the mixed layer than there
8 was in 2006. This drives the observed greater $\delta^3\text{He}$ flux in the 1980s compared to the 2000's.

9
10 Fig. 5. The ^3He flux as a function of fractional year for the 2003-2006 time period
11 (red) and the 1985-1988 time period (black). The time period between 0 and 0.4 has
12 been replicated from 1 to 1.4 in order to better visualize a seasonal cycle.

8. Tables

Table 1. Fluxes calculated from the flux gauge technique for two different time periods. 1σ uncertainty estimates for each flux is given in parentheses underneath the reported value for each quantity.

Time Period	$\text{NO}_3\text{:}^3\text{He} \times 10^{-3}$ ($\mu\text{mol pmol}^{-1}$)	<i>QuikSCAT Winds</i>		<i>NCEP Winds</i>	
		^3He Flux ($\text{pmol m}^{-2} \text{y}^{-1}$)	NO_3 Flux ($\text{mol m}^{-2} \text{y}^{-1}$)	^3He Flux ($\text{pmol m}^{-2} \text{y}^{-1}$)	NO_3 Flux ($\text{mol m}^{-2} \text{y}^{-1}$)
2003-2006	82.9 (2.1)	7.9 (1.7)	0.65 (0.14)	8.3 (1.8)	0.69 (0.15)
1985-1988	34.5 (1.1)	-- --	-- --	30.4 (5.4)	1.05 (0.2)

Table 2. The fractional uncertainty caused by different sources in the calculations of nitrate flux for the 2003-2006 time period.

Source of Error	% uncertainty	Reference or method
Air-sea gas exchange	14%	Stanley et al., 2009
Dynamic solubility equilibrium		
- From diffusivity	10%	calculated with range from Bourg and Sposito, 2008
- From bubble treatment	13%	calculated with range of Gas Exchange from Stanley et al., 2009
Measurement error	5%	Integration of error at each time point
$\text{NO}_3\text{:}^3\text{He}$ Slope	2.5%	Type 2 regression
Tritium correction	1%	Tritium measurement uncertainty propagated to ^3He flux

9. Figures

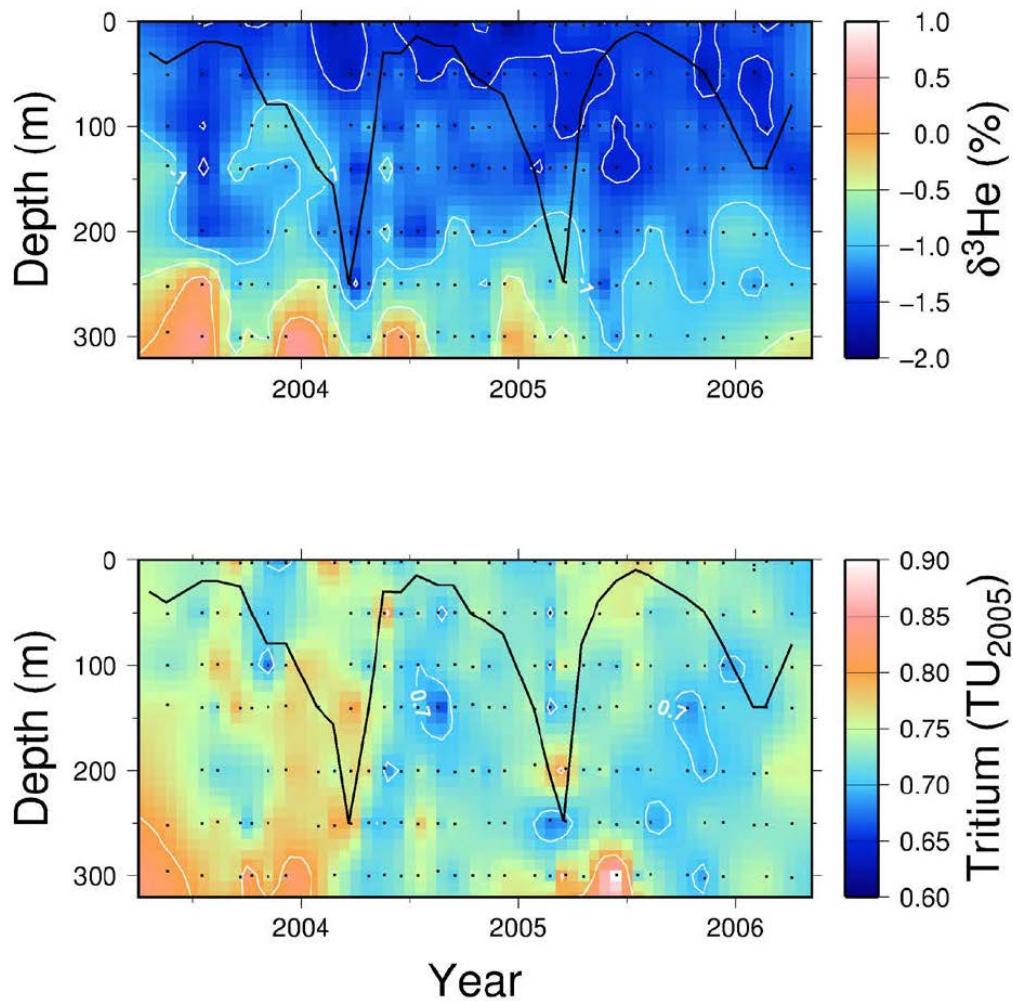


Fig. 1. A time series of helium isotope ratio anomaly (in percent) relative to the atmospheric $^3\text{He}/^4\text{He}$ ratio (upper panel) and tritium (in Tritium Units) decay corrected to January, 2005 (lower panel) at the Bermuda Atlantic Time Series Site in the North Atlantic near Bermuda. Sampling, designated by black dots, was approximately monthly over the ~3 year period. The black line is the mixed layer depth estimated from the CTD data.

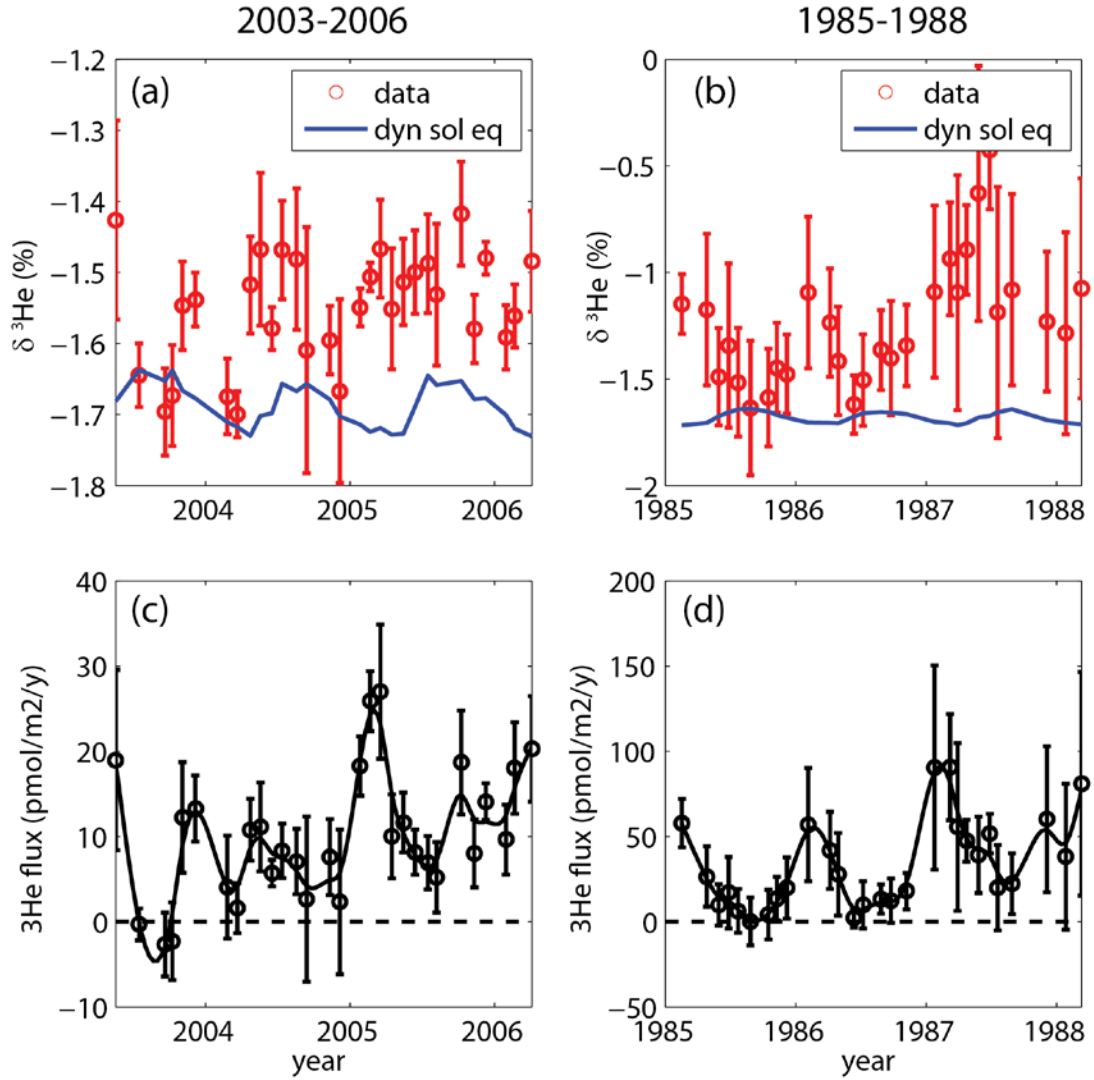


Fig. 2. Mixed layer $\delta^3\text{He}$ data from (a) 2003-2006 and (b) 1985-1988 as well as the dynamic solubility equilibrium for $\delta^3\text{He}$. Error bars represent standard error of multiple measurements within the mixed layer. Fluxes of ^3He calculated from the data for (c) 2003-2006 and (d) 1985-1988. Note the difference in scales on the y-axes for the two time periods.

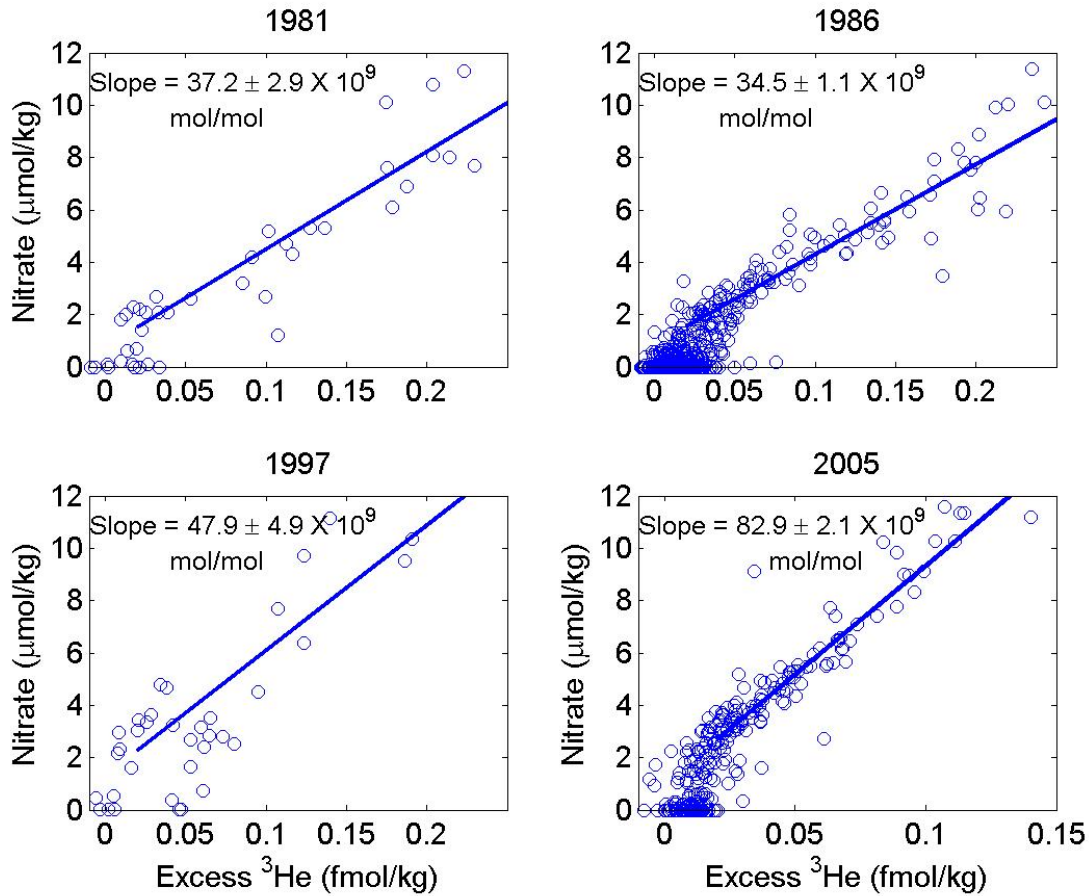
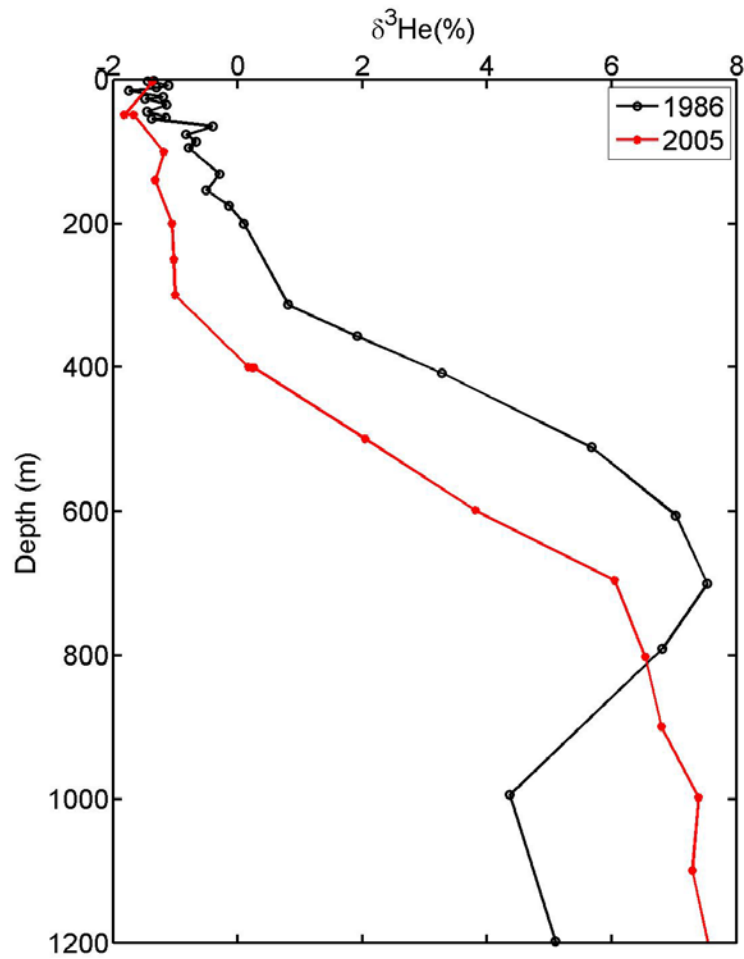


Fig. 3. The observed relationship between excess (tritiogenic) ^3He and dissolved inorganic nitrate near Bermuda at four points in time. The 1986 and 2005 relations are based on approximately 3 year time series occupations near Bermuda (the former at Hydrostation S and the latter at BATS). The 1981 and 1997 data sets are from cruise stations within ~ 500 km of the site. Only samples with potential density anomalies less than 26.8 kg m^{-3} are plotted and used. Note the “water fall” effect at low ^3He and nitrate concentrations in the euphotic zone, where the two tracers become uncoupled due to differing boundary conditions. The straight lines, from which the slopes are obtained, are type II linear regressions of points with nitrate concentrations in excess of $2 \text{ } \mu\text{mol kg}^{-1}$. The lower bound nitrate limit was chose to avoid the tracer-decoupled points.

1

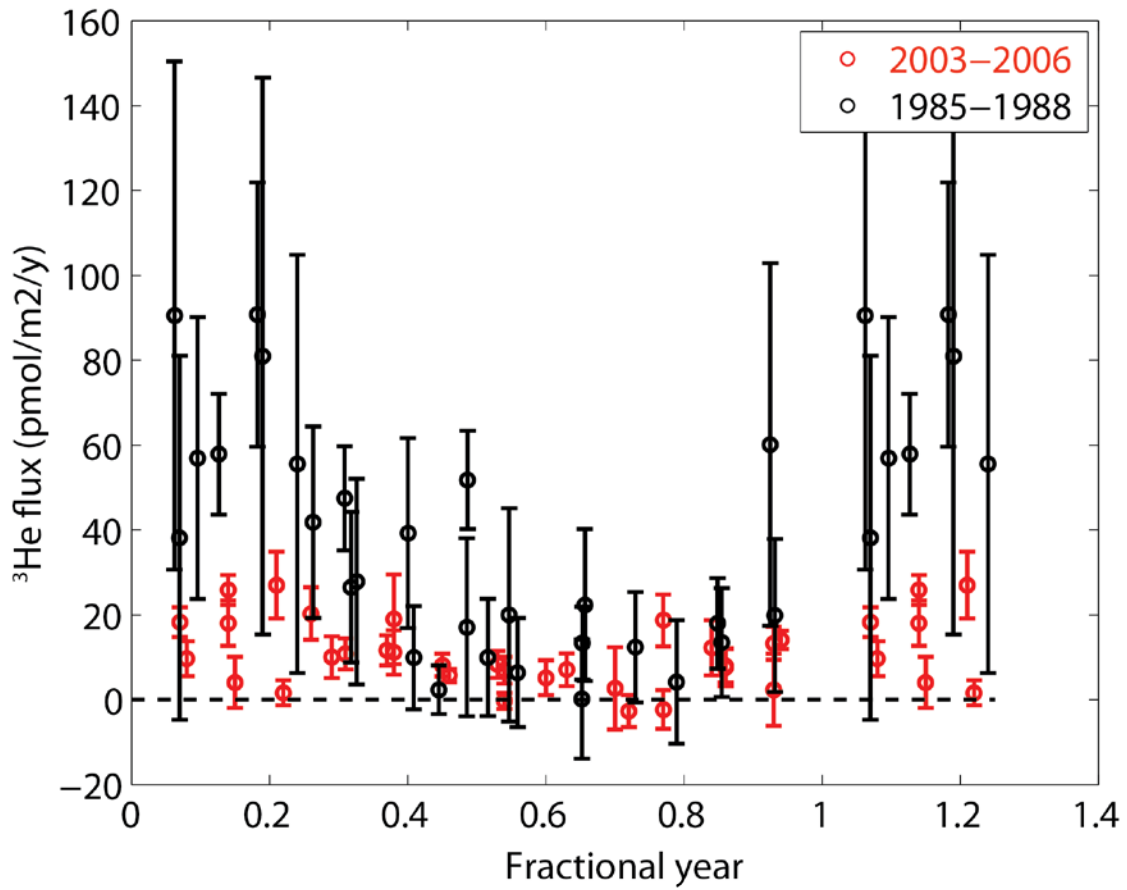


2

3 Fig. 4. Representative profiles of $\delta^3\text{He}$ in the upper 1200 m of the water column in 1986 (black)
 4 and 2003-2006 (red). The profiles illustrate that in 1986 there was much higher $\delta^3\text{He}$ in the main
 5 thermocline and a larger gradient between the thermocline and the mixed layer than there was in
 6 2006. This drives the observed greater ^3He flux in the 1980s compared to the 2000's.

7

1



2

3

4

5

6

7

Fig. 5. The ^3He flux as a function of fractional year for the 2003–2006 time period (red) and the 1985–1988 time period (black). The time period between 0 and 0.4 has been replicated from 1 to 1.4 in order to better visualize a seasonal cycle.

7